

Surface, Physicomechanical, and Chemical Properties of Wood/Polypropylene Composites from Various Formulations after Accelerated Weathering

Yi-Hung Wu,^a Wei-Cheng Chao,^b Tsu-Hsien Yang,^b Feng-Cheng Chang,^{c,*} and Te-Hsin Yang^{b,*}

Accelerated weathering experiments were used to examine the durability and changes in various attributes of WPCs manufactured with the same wood powder size but varying polypropylene-to-wood ratios. Results from the accelerated weathering test revealed color changes, and each attribute generally declined with longer weathering times. In terms of mechanical qualities, the preservation of strength and stiffness increased with increasing plastic content. More wood flour led to higher moisture uptake in frequent humidity fluctuations and high temperatures. It also caused swelling as well as subsequent cracks. Such surface damage could result in faster weathering and worse mechanical qualities. Additionally, the carbonyl index and the functional groups on the surface of WPCs underwent significant changes with increased weathering time.

DOI: 10.15376/biores.18.3.6348-6363

Keywords: Wood-plastic composites; Recycled polypropylene; Accelerated weathering

Contact information: a: Experimental Forest, National Chung Hsing University, Taichung, Taiwan, 145 Xingda Rd., Taichung 40227, Taiwan; b: Department of Forestry, National Chung Hsing University, 145 Xingda Rd., Taichung 40227, Taiwan; c: School of Forestry and Resource Conservation, National Taiwan University; #1, Sec. 4, Roosevelt Rd., Taipei 106319, Taipei, Taiwan;

*Corresponding authors: fcchang@ntu.edu.tw; tehsinyang@nchu.edu.tw

INTRODUCTION

In recent years, wood-plastic composites (WPCs) have been widely used in many outdoor facilities and buildings. The WPCs composition contains a mixture of various proportions of wood fiber and plastic. In addition to wood, many other natural fibers, such as wheat, kenaf, cornstalk, rice husk, jute, hemp, and other agriculture residual, have also been investigated (Yao *et al.* 2008; Chang *et al.* 2010; Turku *et al.* 2018; Dayo *et al.* 2020), and there is also some study of partial addition of carbon and glass fiber (Valente *et al.* 2011; Durmaz *et al.* 2021) or construction wastes (Bakshi *et al.* 2021) into WPCs. The benefit of mixing wood fiber with plastics is attributed to lower cost and lower density, and usually wood fiber provides better stiffness and other mechanical properties for WPCs (Takatani *et al.* 2000; Stark and Rowlands 2003; Wolcott 2003; Chowdhury and Wolcott 2007; Chang *et al.* 2010; Leu *et al.* 2012; Chang *et al.* 2016). However, because natural fibers and plastic are organic materials, the materials are susceptible to various environmental factors that cause deterioration and affect the use of the materials outdoors. Therefore, WPCs' durability with natural fibers as the raw material needs practical verification.

The quality and properties of WPCs products change with time used, particularly under various weathering conditions, as indicated in some previous related accelerated weathering studies. Regarding raw materials, Turku *et al.* (2018) mentioned that weathering had a more substantial impact on WPCs made from plastic waste than virgin material. Stark *et al.* (2004) suggested that the weathering resistance of WPC products varied with different manufacturing methods and was reduced with high moisture during the exposure of wood fiber. Turku *et al.* (2018) also stated that absorbed water in WPCs weakened interfacial interaction in the composite, leading to the degradation of the mechanical properties. Moreover, the damaged surfaces of WPCs could be observed after weathering, and the density of WPCs decreased (Stark and Matuana 2007). Further, after weathering, these damaged and rough surfaces affect WPCs' elongation at maximal strength (Badji *et al.* 2017). On the other hand, Bakshi *et al.* (2021) mentioned adding some calcium-rich waste resources enhanced the properties of WPCs after accelerated UV weathering exposure with potential for civil engineering applications.

In contrast to photooxidation, plastic may have more severe degradation than wood fiber does when exposed to ultraviolet (UV) light (La Mantia and Morreale 2008), and using additives to improve the photodegradation has also been studied (Peng *et al.* 2015; Li *et al.* 2017). Fabiyi and McDonald (2010) found that after accelerated weathering, the color changes of WPCs increased significantly after 1200 h of weathering and then decreased, and other studies suggested that using additives, such as carbon black, red pottery clay, or UV absorber, could improve the color stability (Li *et al.* 2017; Nguyen *et al.* 2018; Turku *et al.* 2018). Moreover, Çavdar *et al.* (2021) indicated that addition of ammonium zeolite in polymer matrix prevented loss in gloss during weathering period.

In addition to physical and surface properties, several previous studies indicated that the photodegradation of plastics and wood induced the mechanical properties of WPCs to decrease with the increasing accelerated weathering times (Peng *et al.* 2014; Turku and Kärki 2016; Turku *et al.* 2018). Although some results showed insignificant change in the early stage of the weathering, the mechanical properties would eventually decrease with the weathering time. Moreover, moisture infiltration influenced interface properties between wood and plastics (Li 2000; Stark and Matuana 2004; Stark *et al.* 2004; Mantia and Morreale 2008).

Regarding surface chemistry, Stark and Matuana (2004) conducted accelerated weathering tests for WPCs and indicated that carbonyl and vinyl group content increased with the increasing weathering time in the early weathering stage. However, after 1000 h weathering, the increasing trend of the vinyl group gradually slowed down, whereas the content carbonyl group continuously increased. Nguyen *et al.* (2018) found that WPCs' carbonyl and ester groups increased after 1000 h UV exposure. Previous studies also mentioned that WPCs would oxidize after accelerated weathering, and polysaccharides and lignin in wood would degrade with weathering time (Fabiyi and McDonald 2010; Peng *et al.* 2015).

Contrastingly, several studies adopted long-term outdoor weathering tests to evaluate the properties changes under practical use. Catto *et al.* (2017) showed that the WPCs with longer exposure to natural weathering presented significant color change, increased carbonyl index, and wood loss on weathered WPC surfaces, suggesting climatic conditions affect the characteristics of WPCs. Kiguchi *et al.* (2007) indicated that color differentials and brightness of WPCs increased and achieved the maximum value after outdoor weathering for 3 months. Yang *et al.* (2015) performed a year-round outdoor weathering test and monitored the WPCs' long-term dynamic changes in physical and

mechanical properties. They found that the degradation rates of various properties were higher than the other literature values, which is most likely due to higher sunlight intensity and heavier rainfall in the tested subtropical regions, implying that the application conditions influence the lifespan of WPCs products. Moreover, polymeric matrices would resist natural weathering differently (Ratanawilai and Taneerat 2018).

This study primarily examined the weather resilience of WPC, where the plastic was made from recycled polypropylene containers, and the wood powder was primarily made from sawdust produced during wood manufacturing. The present circular economy debate is consistent with the idea of putting a priority on resource reuse and minimizing waste. The value of this work is crucial because if the produced WPC may benefit from weather resistance and carbon storage, this implies benefits for both carbon sequestration and carbon replacement. Particularly in Taiwan, the average annual demand for wood consumption is about 4 to 6 million m³, and the generated waste is approximately 20 to 30%. A significant amount of wood waste was produced, and approximately 204,000 metric tons of plastic containers were recycled. In the past ten years, Taiwan has imported an average of about 562,313 m³ of logs, 1,252,590 m³ of lumber, and 1,200,907 m³ of veneer and plywood. The efficient utilization of these recycled resources is therefore advantageous for long-term sustainability.

At present, WPC is commonly used as building materials in outdoor landscape facilities, platforms and trails in Taiwan, but the deformation and fading of WPC are often seen outdoors. Therefore, this study employed accelerated weathering tests to assess the weathering influence on various properties of extruded WPCs of various formulations to thoroughly investigate various WPC properties during weathering. To explore the observed time-dependent changes of WPCs under harsh conditions, samples are taken at various times during the weathering period to analyze the changes in various physical, mechanical, and chemical properties during the accelerated weathering process. The results of this study would be the referential basis for the development and use of WPC in Taiwan.

EXPERIMENTAL

Materials

The recycled S-P-F wood flour was sawdust collected in wood processing, provided by Bestwood Co., Ltd., Taiwan. The recycled polypropylene (PP) (Code ST868 M) pellets were prepared from recycled plastic containers by Shih-Jie Enterprise Co., Ltd., Taiwan. The additives, including maleic anhydride polypropylene (MAPP) as the coupling agent and zinc stearate ($\text{Zn}(\text{C}_{18}\text{H}_{35}\text{O}_2)_2$, ZnSt) as the lubricant, were prepared by the Plastics Industry Development Center (PIDC), Taichung, Taiwan. Before the experiment, the wood flours were oven-dried at 105 °C for 24 h to decrease the moisture content to 2% or lower and then screened to remove the large particles by an automated mesh. Wood flours with a size smaller than 125 μm were used in this study.

Sample Production

The formulations of the produced WPC products in this study are shown in Table 1. The groups were labeled based on polypropylene contents (*e.g.*, PP70 means approximately 70% polypropylene content in the mixture). The constituents were first compounded using a compounder under a mixing rate of 50 rpm, 180 °C for 15 min, then pelletized for further extrusion. Before extrusion, those pellets were dried at 105 °C for 24

h. Next, the WPC pellets were fed directly through a counter-rotating twin-screw extruder at a screw speed of 5 rpm with temperatures ranging from 170 to 200 °C. Finally, the WPCs solid deck boards were produced through a 25 mm (thickness) × 140 mm (width) solid profile die and cooled through a water bath tank at a rate of 0.7 to 0.8 m/min. The formulations and processing conditions are selected based on the results from Leu *et al.* (2012).

Table 1. Material Formulations of Tested Wood-Plastic Composites

Groups	Wood Flour Size (µm)	Coupling Agent (wt%)	Lubricant (wt%)	Wood/Plastic Ratio (wt%/wt%)
PP70	< 125	3	3	28.2/65.8
PP60	< 125	3	3	37.6/56.4
PP50	< 125	3	3	47.0/47.0
PP40	< 125	3	3	56.4/37.6

Note: Coupling agent: Maleated polypropylene (MAPP); Lubricant: Zinc stearate (ZnSt); Plastics: Polypropylene

Accelerated Weathering

Referring to ASTM G53-96 (2000), the produced WPC specimens were tested in a QUV accelerated weathering tester (QUV/se, Q-Lab corporation, Westlake, OH, USA) for 2000 h, and the light source is a UVA-340 lamp, which gives the simulation of sunlight in the critical short wavelength region from 295 to 365 nm, and the irradiance was 0.89 W/m² at 340 nm wavelength. The cycle of UV exposure for 8 h at 70 °C and condensation for 4 h at 50 °C was set to simulate the effect of more extended periods in natural conditions on WPCs' physical and mechanical properties. During the weathering period, specimens at different time points evaluated various properties changes during the degradation process.

Material Properties

Morphology

At different time points after accelerated weathering, the surface morphology of the produced WPCs samples was observed using scanning electron microscopy (SEM). The surface of the specimens was sputter-coated with gold before observation in SEM (S-4800; HITACHI, Tokyo, Japan).

Density and moisture content

The density of WPCs was measured according to ASTM D1037-12 (2020). The sample measured 40 × 13.5 × 4.5 mm³. The air-dry weight and size of specimens were measured first and then oven-dried at 103 ± 2 °C for 1 week so that air-dry moisture and density could be obtained based on the following,

$$\text{Density (g/cm}^3\text{)} = \frac{l_{\text{air}}}{LWT} \quad (1)$$

$$\text{Moisture content (\%)} = \frac{l_{\text{air}} - l_{\text{dry}}}{l_{\text{dry}}} \times 100 \quad (2)$$

where *L* is the length (mm); *W* is the width (mm); *T* is the thickness (mm); *l*_{air} is the air-dry weight (g); and *l*_{dry} is the oven-dry weight (g). Moreover, 10 specimens were taken at different time points after accelerated weathering, and the density and moisture contents were measured similarly.

Thickness swelling and water absorption

The measurement was conducted based on ASTM D1037-12 (2020), and the size of the specimen measured $80 \times 13.5 \times 4.5 \text{ mm}^3$. The air-dry weight and thickness of the specimen were measured first and then immersed in a water bath for 24 h and measured the weight and thickness of the specimen. As a result, the thickness swell and water absorption rate could be obtained based on the following equations,

$$\text{Thickness swelling (\%)} = \frac{T_{\text{after}} - T_{\text{air}}}{T_{\text{air}}} \times 100 \quad (3)$$

$$\text{Water absorption (\%)} = \frac{l_{\text{after}} - l_{\text{air}}}{l_{\text{air}}} \times 100 \quad (4)$$

where l_{air} is the air-dry weight (g); l_{after} is the weight (g) after 24 h water absorption; T_{air} is the air-dry thickness (mm); and T_{after} is the thickness (mm) after 24 h water absorption. Moreover, 10 specimens were taken at different time points after accelerated weathering, and the thickness swelling and water absorption were measured similarly.

Colorimetric analysis

The surface color of the WPC specimens was measured with a spectrophotometer (CM-3600d, Minolta, Tokyo, Japan) according to the CIE $L^*a^*b^*$ color system, and the lightness (L^*) and chromaticity coordinates (a^* and b^*) were measured for 20 replicates. The illuminant was D65, and the observer angle was 10° , while the diameter of the observation window was 8 mm. The total color change ΔE^* was calculated with the following Eqs. 5 through 8,

$$\Delta L^* = L^*_{\text{T}} - L^*_{\text{0}} \quad (5)$$

$$\Delta a^* = a^*_{\text{T}} - a^*_{\text{0}} \quad (6)$$

$$\Delta b^* = b^*_{\text{T}} - b^*_{\text{0}} \quad (7)$$

$$\Delta E^* = [(\Delta L^*)^2 + (\Delta a^*)^2 + (\Delta b^*)^2]^{1/2} \quad (8)$$

where ΔL^* , Δa^* , and Δb^* are the differences between initial values (L^*_{0} , a^*_{0} , and b^*_{0}) and that after accelerated weathering for a certain time (L^*_{T} , a^*_{T} , and b^*_{T}), respectively. Moreover, specimens were taken at different time points after accelerated weathering, and the color difference were similarly measured.

Surface carbonyl index

An attenuated total reflectance Fourier-transform infrared spectroscopy (ATR-FTIR, PerkinElmer Spectrum 100, Waltham, MA, USA) was used to detect the surface functional group of WPCs taken before and after accelerated weathering at different weathering times to understand the change of the functional groups and the carbonyl content of WPCs after accelerated weathering. Spectra were recorded from 4000 to 650 cm^{-1} and at a 4 cm^{-1} spectral resolution with 32 co-adding scans. Furthermore, the carbonyl index could be calculated and determined by comparing the band intensity of the carbonyl group measured at 1735 cm^{-1} with that of the methyl group at 2916 cm^{-1} , according to the following equation (Stark and Matuana 2004, 2007),

$$\text{Carbonyl index} = (I_{1735}/I_{\text{PP}}) \quad (9)$$

where I_{PP} is the intensity of the specific absorption band of PP (2916 cm^{-1}); I_{1735} is the intensity of the carbonyl absorption band (1735 cm^{-1}). On the other hand, the changing of lignin after accelerated weathering would also be observed on the FTIR spectrum.

Mechanical properties

Three-point bending tests were conducted according to ASTM D790-17 (2017), using a Shimadzu AG-250KNI universal-type testing machine (Kyoto, Japan). The specimen size was measured at $130 \times 13.5 \times 4.5\text{ mm}^3$. The flexural test was conducted with 10 replicates. The modulus of rupture (MOR) and the modulus of elasticity (MOE) were obtained based on the following Eqs. 10 and 11, respectively,

$$\text{MOR} = \frac{3PL}{2bh^2} \quad (10)$$

$$\text{MOE} = \frac{\Delta PL^3}{4\Delta Ybh^3} \quad (11)$$

where L is the span (mm); b and h are the width (mm) and thickness (mm) of the specimen, respectively; P is the maximum load (N); A is the cross-section area (mm^2), ΔP is the load difference under the promotional limit, and ΔY is the deflection difference associated with ΔP .

Mechanical properties retention

During the accelerated weathering tests, samples were taken at different time points, and then 3-point bending tests were conducted, as above-mentioned, to obtain MOE and MOR values to evaluate the weathering-resistant capacity of the produced WPCs. The MOR and MOE retention could be obtained based on the following Eqs. 12 and 13,

$$\text{Retained MOR ratio (\%)} = (\text{MOR}_t/\text{MOR}_o) \times 100 \quad (12)$$

$$\text{Retained MOE ratio (\%)} = (\text{MOE}_t/\text{MOE}_o) \times 100 \quad (13)$$

where MOR_t (MPa) and MOE_t (GPa) were the MOR (MPa) and MOE (GPa) values at different time points after accelerated weathering, respectively, while MOR_o and MOE_o were the MOR and MOE values obtained before weathering, respectively.

Statistical Analysis

Comparisons by different factors were discussed with analysis of variance (ANOVA, $\alpha = 0.05$) using SPSS 20 (IBM Corporation, Armonk, NY, USA) to test the significant effect. The Tukey test (confidence level 95%) was also conducted to test significant differences between groups.

RESULTS AND DISCUSSION

Morphology

Figure 1 shows the SEM photos of surface conditions of different WPCs groups after various accelerated weathering times. In the first 500 h of weathering, surfaces of all groups did not appear to have significant changes; however, after 1000 h of accelerated weathering, accompanied by matrix cracks, coarse surfaces of all groups started to appear,

and cracks between wood flour and PP could be observed. Moreover, when the weathering time reached 2000 h, the deterioration of the plastic becomes more serious, which may be explained by the photooxidation of PP induced by UV irradiation. The PP molecular chains may break, be reformed, and crystallized during accelerated weathering, and cause internal structure shrinkage, resulting in external damage.

In addition, PP40 showed more severe crack damages than others because PP40 contained more wood flour, and the moisture uptake could be higher than others under frequent humidity changing and high-temperature environments, resulting in wood flour swelling and inducing more following cracks. Turku and Kärki (2016) also mentioned that UV irradiation and the presence of water would result in cracks on the WPC surfaces.

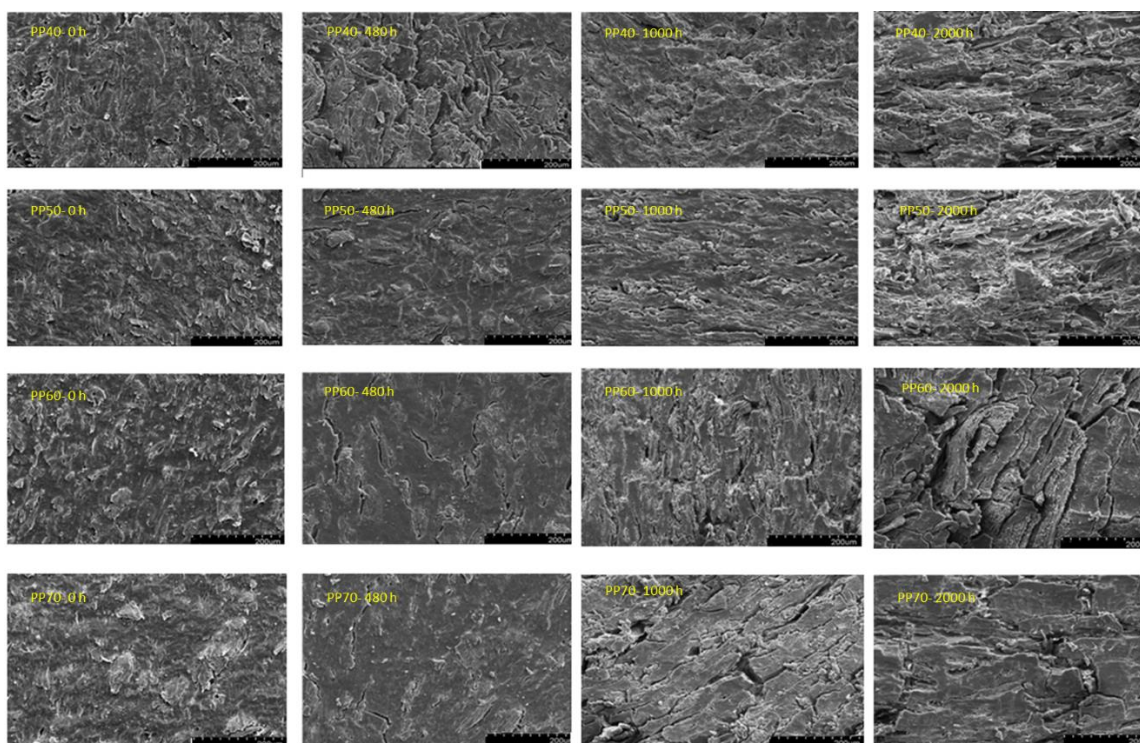


Fig. 1. SEM images of the surface of WPCs during 2000 h accelerated weathering

Color Changes

Four color indexes were plotted over the weathering time in Fig. 2. Generally, the change in the color of the WPCs can be seen as the deterioration of the material. Part of Figure shows that L^* decreased during the first 100 h and then increased to 1000 h accelerated weathering with time. The L^* of each WPCs group started to increase significantly in the beginning and changed with the weathering time, but no specific trend was found after 1000 h accelerated weathering, which is consistent with the results of the accelerated test conducted by Stark *et al.* (2004) and Kiguchi *et al.* (2007). In addition, Fabiyi and McDonald (2010) also mentioned that the values ΔE^* and L^* of WPCs increased significantly after 1200 h of weathering and then decreased. Moreover, according to Fig. 2-(b) and 2-(c), a^* and b^* of all WPCs increased with the accelerated weathering time, showed a rising trend initially, and then decreased.

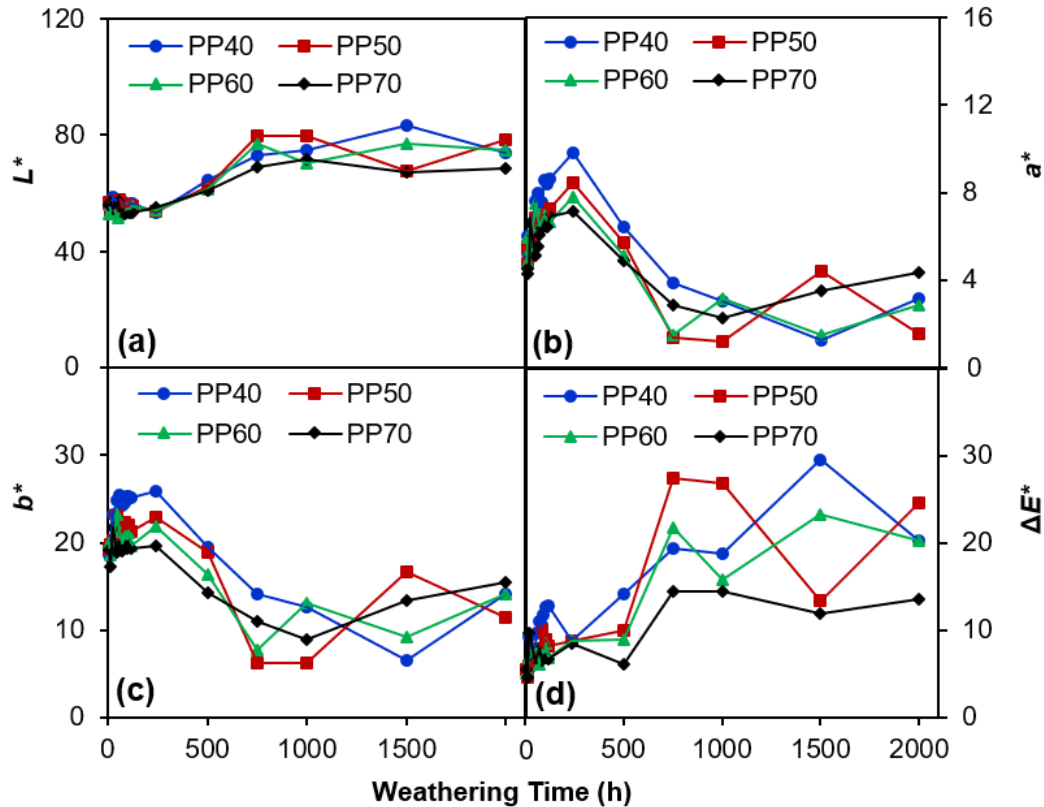


Fig. 2. Change of various color parameters of WPCs after accelerated weathering for 2000 h: (a): L^* , (b): a^* , (c): b^* , (d): ΔE^*

Ultraviolet irradiation usually influences surface morphology, and exposure to UV for a specific time would whiten the surface of WPCs (Li *et al.* 2014). Peng *et al.* (2015) indicated that the color fading in the composites results from the photodegradation of lignin, which is more sensitive to UV light due to chromophoric groups on its structure (Peng *et al.* 2014). It is speculated that the lignin in the early stage of degradation produced quinones due to photooxidation chromophores (Ndiaye *et al.* 2008), causing yellowing in WPCs, and then the water generated by the condensation cycle rinses out these chromophores, shifting the color change of WPCs to blue. Thus, the change of a^* is affected by the degradation of lignin or extracts. In contrast, ΔE^* had a similar change as L^* , implying that the change in ΔE^* was mainly affected by L^* , and among the four WPCs, the color change of PP40 is more considerable than other groups.

Physical Properties

Various physical properties of WPCs after accelerated weathering are shown in Table 2. After accelerated degradation, the density of each WPCs group just had a slightly decreasing trend. In contrast, the moisture content of each group showed an increasing trend with the accelerated weathering time, which also reflected those mentioned above that surface damage might occur during accelerated weathering so that moisture content would increase due to water absorption from those exposed wood flour.

The water absorption and thickness swelling of WPCs may also be inferred similarly. Each WPCs group displayed a rising trend with the accelerated weathering time regarding water absorption capacity after varied accelerated weathering intervals. In

addition to surface deterioration brought on by weathering, the findings could also be affected by the wood flour content; the more wood there is, the more water is absorbed. The content of PP is relatively less to cover the surface of the wood flour, causing a more exposed area of wood flour and inducing more water uptake. Additionally, the dimensional stability was also influenced. Notably, PP40 demonstrated significantly higher moisture content and water absorption than others. Comparatively, PP70 had much less water uptake attributing to a substantially larger plastic content than the other groups.

Table 2. Various Physical Properties of WPCs after Weathering

Properties	Weathering Time (h)	PP40	PP50	PP60	PP70
Density (g/cm ³)	0	1.15 ± 0.01	1.12 ± 0.01	1.07 ± 0.01	1.05 ± 0.01
	24	1.18 ± 0.01	1.15 ± 0.01	1.09 ± 0.02	1.07 ± 0.01
	72	1.18 ± 0.01	1.15 ± 0.01	1.10 ± 0.02	1.05 ± 0.03
	120	1.18 ± 0.01	1.15 ± 0.01	1.10 ± 0.02	1.05 ± 0.03
	480	1.19 ± 0.01	1.14 ± 0.01	1.09 ± 0.01	1.08 ± 0.01
	750	1.18 ± 0.00	1.14 ± 0.01	1.09 ± 0.01	1.07 ± 0.01
	1000	1.16 ± 0.01	1.12 ± 0.01	1.11 ± 0.01	1.06 ± 0.01
	2000	1.15 ± 0.02	1.14 ± 0.01	1.09 ± 0.01	1.05 ± 0.01
Moisture content (%)	0	3.23 ± 0.29	1.45 ± 0.10	1.41 ± 0.11	1.33 ± 0.11
	24	4.95 ± 0.37	5.20 ± 0.55	3.02 ± 0.52	5.40 ± 0.37
	72	6.09 ± 0.50	3.80 ± 0.48	3.41 ± 0.53	3.24 ± 0.37
	120	4.67 ± 0.40	4.56 ± 0.56	4.17 ± 0.40	2.92 ± 0.56
	480	4.81 ± 0.48	3.69 ± 0.58	2.83 ± 0.54	3.46 ± 0.47
	750	6.19 ± 0.41	4.03 ± 0.29	4.20 ± 0.51	4.19 ± 0.46
	1000	4.22 ± 0.48	4.15 ± 0.53	4.24 ± 0.49	2.76 ± 0.49
	2000	6.05 ± 0.53	4.82 ± 0.43	3.44 ± 0.33	3.30 ± 0.56
Water absorption (%)	0	1.81 ± 0.10	0.93 ± 0.14	0.98 ± 0.20	0.57 ± 0.13
	24	2.34 ± 0.17	0.45 ± 0.14	1.11 ± 0.43	0.59 ± 0.14
	72	2.14 ± 0.30	1.31 ± 0.33	1.40 ± 0.13	0.75 ± 0.24
	120	3.93 ± 0.18	0.87 ± 0.41	0.63 ± 0.23	0.50 ± 0.24
	480	4.83 ± 0.19	1.47 ± 0.35	0.43 ± 0.19	0.46 ± 0.18
	750	6.47 ± 0.42	1.78 ± 0.28	1.60 ± 0.18	0.38 ± 0.19
	1000	5.45 ± 0.79	2.03 ± 0.24	0.90 ± 0.19	0.25 ± 0.11
	2000	6.42 ± 0.31	1.83 ± 0.45	2.34 ± 1.35	1.17 ± 0.30
Thickness swelling (%)	0	1.50 ± 0.49	0.69 ± 0.14	0.54 ± 0.26	0.27 ± 0.08
	24	2.28 ± 0.24	0.73 ± 0.12	0.56 ± 0.20	0.46 ± 0.16
	72	2.31 ± 0.29	1.08 ± 0.28	0.74 ± 0.19	0.65 ± 0.22
	120	2.60 ± 0.30	0.84 ± 0.26	0.33 ± 0.19	0.17 ± 0.07
	480	4.62 ± 0.05	0.82 ± 0.28	0.29 ± 0.11	0.26 ± 0.06
	750	4.86 ± 0.70	1.06 ± 0.25	0.46 ± 0.23	0.23 ± 0.11
	1000	3.71 ± 0.11	1.03 ± 0.30	0.25 ± 0.06	0.15 ± 0.06
	2000	6.41 ± 0.27	1.10 ± 0.25	1.01 ± 0.24	0.47 ± 0.20

Mechanical Properties

In general, decreasing flexural strength could be observed with the increasing weathering time (Table 3). The void between wood flour and PP tends to increase after accelerated weathering, showing that the bonding between wood and PP decreases as the

weathering degradation time increases so that the mechanical properties would have inferior performance. Moreover, the statistical analysis revealed significant differences before and after accelerated weathering. In contrast, because the higher PP content covered wood flour, PP70 exhibited better mechanical properties retention, indicating better weathering durability. In contrast, PP40 showed the lowest mechanical properties retention, losing nearly 56% flexural strength. The MOR retention of the various WPCs during accelerated weathering is shown in Fig. 3. The results indicated that lower PP content causes decreasing both physical and mechanical properties. Consequently, the formulation played a critical role in developing durability; the higher the wood flour content, the lower durability.

Table 3. Mechanical Properties of WPCs during 2000 h Accelerated Weathering

Properties	Weathering Time (h)	PP40	PP50	PP60	PP70
MOE (GPa)	0	3.20 ± 0.58 ^{acd}	2.87 ± 0.21 ^a	2.63 ± 0.16 ^{ab}	2.54 ± 0.13 ^a
	24	3.67 ± 0.41 ^{cd}	3.30 ± 0.12 ^{bc}	2.82 ± 0.13 ^{bc}	2.58 ± 0.09 ^{ab}
	72	3.86 ± 0.18 ^d	3.28 ± 0.11 ^{bc}	2.93 ± 0.09 ^c	2.60 ± 0.13 ^{ab}
	120	3.41 ± 0.30 ^{bcd}	3.31 ± 0.12 ^{bc}	2.84 ± 0.12 ^{bcd}	2.55 ± 0.14 ^a
	480	3.35 ± 0.26 ^{bcd}	3.40 ± 0.11 ^c	3.05 ± 0.09 ^d	2.77 ± 0.13 ^b
	750	2.62 ± 0.34 ^{ae}	3.14 ± 0.12 ^b	2.62 ± 0.20 ^a	2.59 ± 0.07 ^{ab}
	1000	3.01 ± 0.35 ^{abe}	2.87 ± 0.15 ^a	2.78 ± 0.14 ^{abc}	2.71 ± 0.14 ^{ab}
	2000	2.61 ± 0.44 ^e	2.78 ± 0.16 ^a	2.57 ± 0.17 ^a	2.66 ± 0.14 ^{ab}
MOR (MPa)	0	24.68 ± 4.66 ^a	28.15 ± 2.53 ^a	31.32 ± 2.26 ^a	33.33 ± 3.76 ^a
	24	18.22 ± 4.79 ^{bc}	27.31 ± 2.82 ^a	27.59 ± 4.27 ^{abcd}	30.32 ± 3.90 ^{ab}
	72	19.83 ± 3.81 ^{ab}	25.15 ± 2.59 ^{ab}	28.19 ± 3.46 ^{abc}	30.39 ± 3.92 ^{ab}
	120	14.75 ± 3.83 ^{bcd}	23.22 ± 1.98 ^{bc}	27.93 ± 3.31 ^{abcd}	27.20 ± 3.94 ^b
	480	16.27 ± 3.74 ^{bcd}	21.90 ± 2.56 ^{bc}	29.06 ± 2.46 ^{ab}	26.33 ± 4.25 ^b
	750	12.49 ± 1.92 ^{cd}	17.01 ± 1.88 ^{de}	23.71 ± 2.23 ^{cd}	29.26 ± 2.11 ^{ab}
	1000	11.74 ± 2.56 ^d	16.04 ± 2.28 ^e	25.22 ± 3.39 ^{bcd}	28.24 ± 3.56 ^{ab}
	2000	10.96 ± 1.99 ^d	19.73 ± 2.07 ^{cd}	23.45 ± 2.74 ^d	30.44 ± 2.91 ^{ab}

Note: The same superscript letter means no significant difference between groups

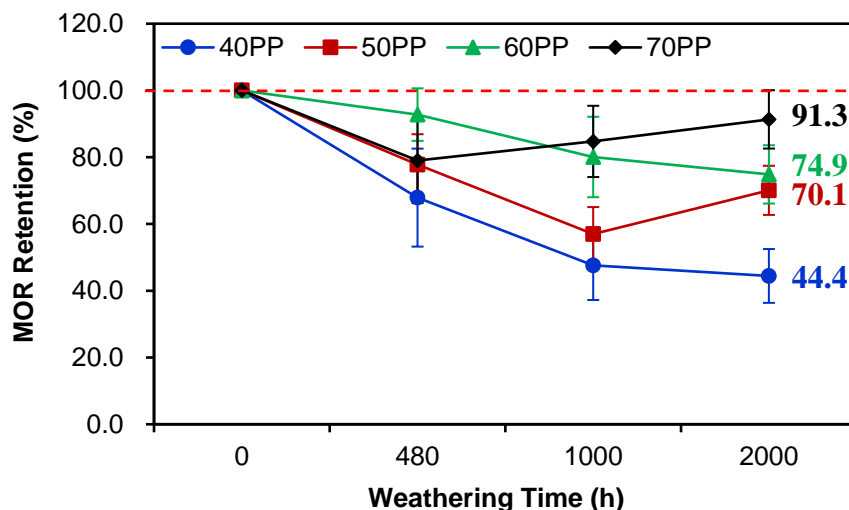


Fig. 3. The MOR retention of WPCs during 2000 h accelerated weathering.

ATR-FTIR and Carbonyl Index

Figure 4 displays the ATR-FTIR spectrum of WPCs during the 2000 h accelerated weathering. The results showed that lignin's specific absorbance band intensities at 1600 and 1510 cm^{-1} decreased with weathering time. Moreover, 1240 cm^{-1} represents the CO stretching absorbance band on the lignin aromatic ring, and the absorbance band intensity was significantly lower after 480 h accelerated weathering. The intensity value of the hydroxyl absorbance band shown at 3050 to 3600 cm^{-1} tended to decrease as the weathering time increased, suggesting the degradation of wood polysaccharides. However, the absorbance band at 1640 cm^{-1} , representing the vinyl group, differed significantly from the outdoor weathering test results (Yang *et al.* 2015). The band value of vinyl absorbance increased with the weathering time, which may be explained why the leaching effect of condensate water in the accelerated weathering test was gentler than the rainwater in the outdoor weathering test so that the degradation products of PP or wood remained more on the surface of the WPCs and therefore be detected. Peng *et al.* (2015) also mentioned that significant changes in the surface chemistry of WPCs occur accompanied by the enrichment of the surface with wood, partly by the photodegradation of the plastic and partly by the movement of wood particles in the cracks to the surface.

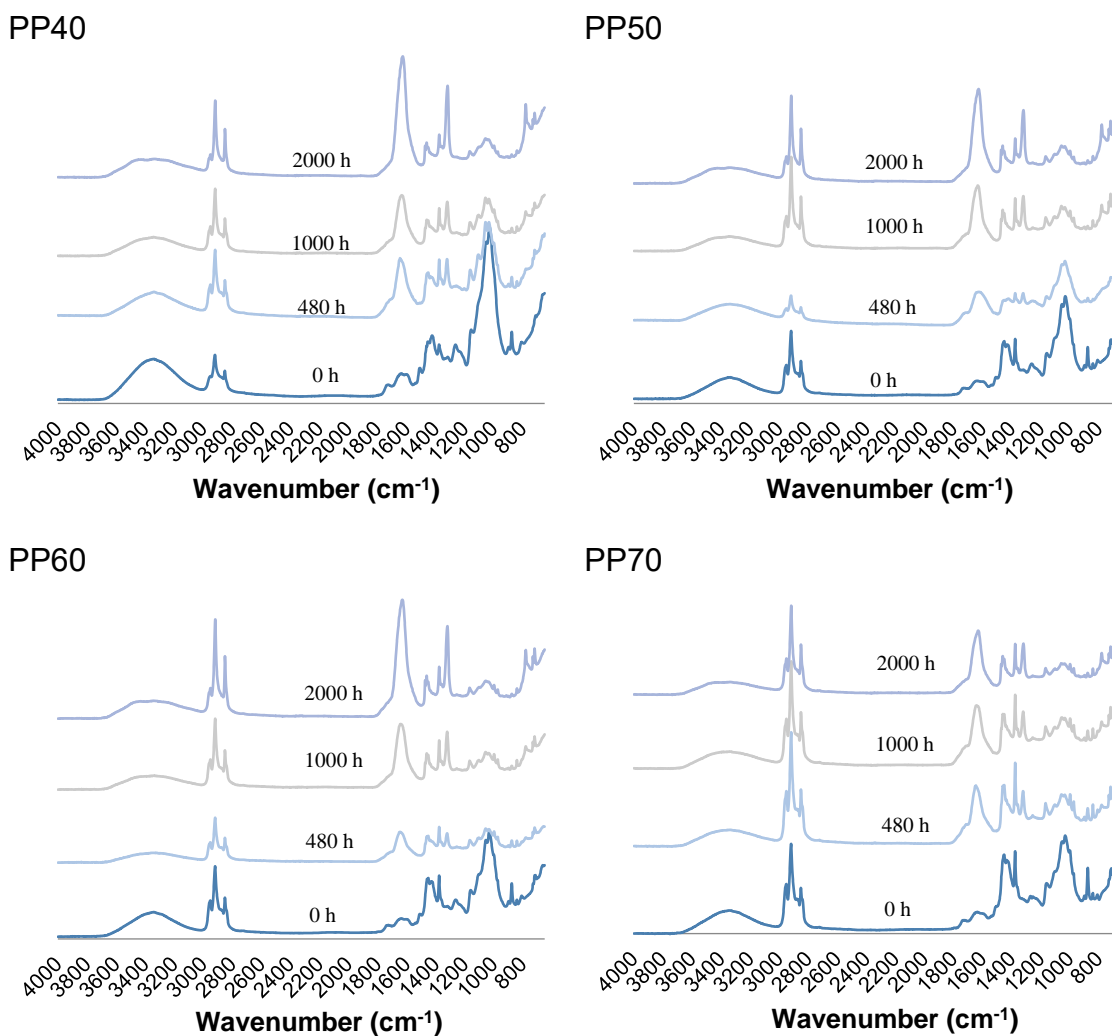


Fig. 4. ATR-FTIR spectra of WPCs after accelerated weathering for 2000 h

Polyolefin experiences two chain fracture reactions, Norrish I and Norrish II, under UV irradiation, affording a carbonyl group and a vinyl group, respectively, and these reactions may cause chain scission or crosslink of the polymer. The increase in the carbonyl and ester group formation for composites after weathering is proportional to the chain scissions occurring in the polymer matrix (Nguyen *et al.* 2018). Figure 5 displays the change of the carbonyl index of the WPCs during the 2000 h accelerated weathering, and the results showed fluctuant changes during the accelerated weathering. Turku *et al.* (2018) indicated that the rate of surface degradation of WPCs could be estimated by the degree of the changes in the carbonyl groups, mainly formed during polymer photodegradation. The carbonyl index of each WPCs group generally showed an upward trend in the early stage of the accelerated weathering due to ascribed residual degradation products of PP or wood that remained on the surface of WPCs, which is also indicated in some previous studies (Stark and Matuana 2004; Ndiaye *et al.* 2008; Fabiyi *et al.* 2008). However, the carbonyl index of each WPCs group decreased in the latter stage due to the more extended period of leaching. Nevertheless, Çavdar *et al.* (2021) indicated the carbonyl index of WPCs may increase after the weathering exposure, differing from this study. However, Çavdar *et al.* (2021) conducted the weathering exposure for a total of 672 h; therefore, only the increase at the early stage was observed in their study.

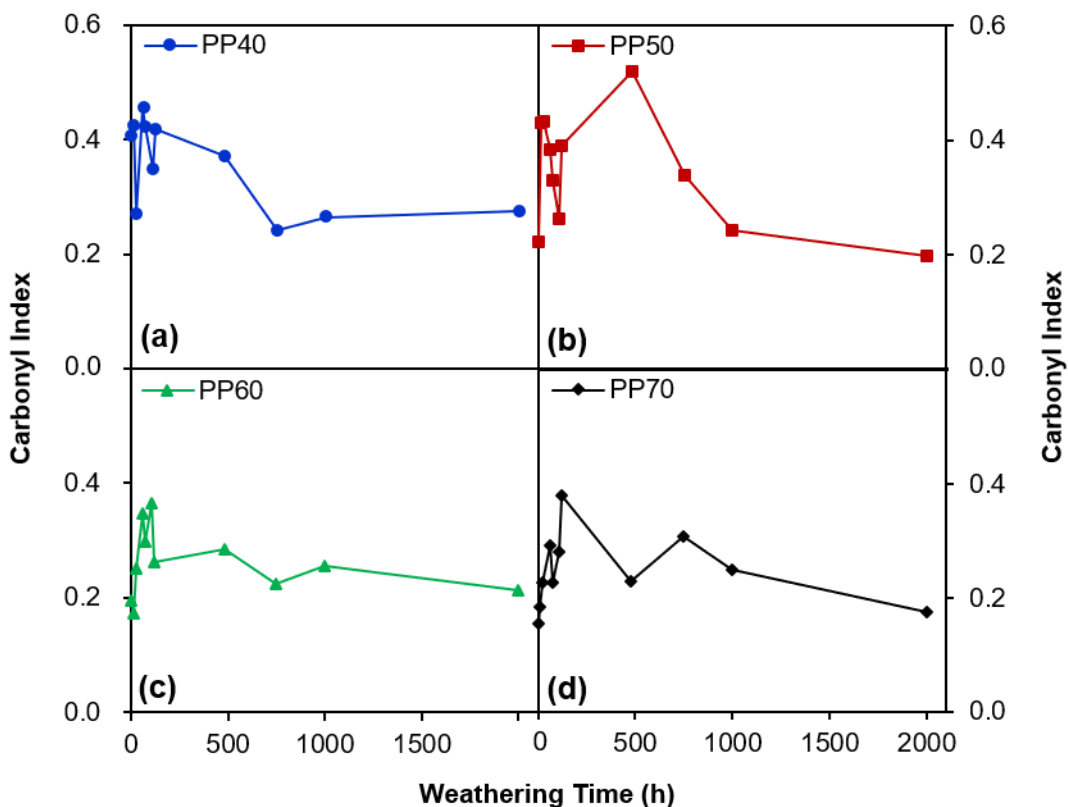


Fig. 5. Change of carbonyl index of WPCs during 2000 h accelerated weathering

CONCLUSIONS

1. The results indicated that the formulation played a critical role in developing durability; a higher wood flour content resulted in lower durability.
2. More wood flour may increase moisture absorption in high-temperature situations and environments with frequent humidity changes. Wood flour may also swell and cause more subsequent cracks, as well as cause surface damage during rapid weathering, and decrease mechanical qualities.
3. The change in the color of the wood-plastic composite (WPC) could be seen as an indication of the deterioration, and the functional groups on the surface of WPCs had a significant change.
4. Due to the prolonged leaching period, the carbonyl index of each WPCs group generally showed a downward trend in the later stages of the accelerated weathering.

ACKNOWLEDGMENTS

The financial support from the National Science and Technology Council (106-2313-B-005-005) for this work is greatly appreciated.

REFERENCES CITED

- ASTM D790-17 (2017). "Standard test methods for flexural properties of unreinforced and reinforced plastics and electrical insulating materials," ASTM International, West Conshohocken, PA, USA.
- ASTM D1037-12 (2020). "Standard test methods for evaluating properties of wood-base fiber and particle panel materials," ASTM International, West Conshohocken, PA, USA.
- ASTM G53-96 (2000). "Practice for operating light-and water-exposure apparatus (fluorescent UV-condensation type) for exposure of nonmetallic materials," ASTM International, West Conshohocken, PA, USA.
- Badji, C., Soccalingame, L., Garay, H., Bergeret, A., and Bénézet, J.-C. (2017). "Influence of weathering on visual and surface aspect of wood plastic composites: Correlation approach with mechanical properties and microstructure," *Polym. Degrad. Stabil.* 137, 162-172. DOI: 10.1016/j.polymdegradstab.2017.01.010
- Bakshi, P., Pappu, A., Bharti, D. K., and Patidar, R. (2021). "Accelerated weathering performance of injection moulded PP and LDPE composites reinforced with calcium rich waste resources," *Polym. Degrad. Stabil.* 192, 109694. DOI: 10.1016/j.polymdegradstab.2021.109694
- Catto, A. L., Montagna, L. S., and Santana, R. M. C. (2017). "Abiotic and biotic degradation of post-consumer polypropylene/ethylene vinyl acetate: Wood flour composites exposed to natural weathering," *Polym. Composite* 38(3), 571-582. DOI: 10.1002/pc.23615

- Çavdar, A. D., Tomak, E. D., Torun, S. B., and Arpacı, S. S. (2021). "Accelerated weathering resistance of high-density polyethylene composites reinforced with microcrystalline cellulose and fire retardants," *J. Build. Eng.* 39, 102282. DOI: 10.1016/j.jobe.2021.102282
- Chang, F.-C., Lam, F., and Englund, K. R. (2010). "Feasibility of using mountain pine beetle attacked wood to produce wood-plastic composites," *Wood Fiber Sci.* 42(3), 388-397.
- Chang, F.-C., Kadla, J. F., and Lam, F. (2016). "The effects of wood flour content and coupling agent on the dynamic mechanical and relaxation properties of wood-plastic composites," *Eur. J. Wood Wood Prod.* 74(1), 23-30. DOI:10.1007/s00107-15-0962-5
- Chowdhury, M. A., and Wolcott, M. P. (2007). "Compatibilizer selection to improve mechanical and moisture properties of extruded wood-HDPE composites," *Forest Prod. J.* 57(9), 46-53.
- Dayo, A. Q., Babar, A. A., Qin, Q.-r., Kiran, S., Wang, J., Shah, A. H., Zegaoui, A., Ghouti, H. A., and Liu, W.-b. (2020). "Effects of accelerated weathering on the mechanical properties of hemp fibre/polybenzoxazine based green composites," *Compos. Part A-Appl. S* 128, 105653. DOI: 10.1016/j.compositesa.2019.105653
- Durmaz, S., Erdil, Y. Z., and Ozgenc, O. (2021). "Accelerated weathering performance of wood-plastic composites reinforced with carbon and glass fibre-woven fabrics," *Color. Technol.* 138(1), 74-81. DOI: 10.1111/cote.12572
- Fabiyi, J. S., McDonald, A. G., Wolcott, M. P., and Griffiths, P. R. (2008). "Wood plastic composites weathering: Visual appearance and chemical changes," *Polym. Degrad. Stabil.* 93(8), 1405-1414. DOI: 10.1016/j.polymdegradstab.2008.05.024
- Fabiyi, J. S., and McDonald, A. G. (2010). "Effect of wood species on property and weathering performance of wood plastic composites," *Compos. Part A-Appl. S* 41(10), 1434-1440. DOI: 10.1016/j.compositesa.2010.06.004
- Kiguchi, M., Kataoka, Y., Matsunaga, H., Yamamoto, K., and Evans, P. D. (2007). "Surface deterioration of wood-flour polypropylene composites by weathering trials," *J. Wood Sci.* 53, 234-238. DOI: 10.1007/s10086-006-0838-8
- La Mantia, F. P., and Morreale, M. (2008). "Accelerated weathering of polypropylene/wood flour composites," *Polym. Degrad. Stabil.* 93(7), 1252-1258. DOI: 10.1016/j.polymdegradstab.2008.04.006
- Leu, S.-Y., Yang, T.-H., Lo, S.-F., and Yang, T.-H. (2012). "Optimized material composition to improve the physical and mechanical properties of extruded wood-plastic composites (WPCs)," *Constr. Build. Mater.* 29, 120-127. DOI: 10.1016/j.conbuildmat.2011.09.013
- Li, R. (2000). "Environmental degradation of wood-HDPE composite," *Polym. Degrad. Stabil.* 70(2), 135-145. DOI: 10.1016/S011-3910(00)00099-9
- Li, H., Zhang, Z., Song, K., Lee, S., Chun, S.-J., Zhou, D., and Wu, Q. (2014). "Effect of durability treatment on ultraviolet resistance, strength, and surface wettability of wood plastic composite," *Bioresources* 9(2), 3591-3601. DOI: 10.15376/biores.9.2.3591-3601
- Li, Q., Gao, X., Cheng, W., and Han, G. (2017). "Effect of modified red pottery clay on the moisture absorption behavior and weatherability of polyethylene-based wood-plastic composites," *Materials* 10(2), 111-127. DOI: 10.3390/ma10020111

- Ndiaye, D., Fanton, E., Morlat-Therias, S., Vidal, L., Tidjani, A., and Gardette, J. L. (2008). "Durability of wood polymer composites: Part 1. Influence of wood on the photochemical properties," *Compos. Sci. Technol.* 63(13), 2779-2784. DOI: 10.1016/j.compscitech.2008.06.014
- Nguyen, V. D., Hao, J., and Wang, W. (2018). "Ultraviolet weathering performance of high-density polyethylene/wood-flour composites with a basalt-fiber-included shell," *Polymers* 10(8), 831-842. DOI: 10.3390/polym10080831
- Peng, Y., Liu, R., Cao, J., and Chen, Y. (2014). "Effects of UV weathering on surface properties of polypropylene composites reinforced with wood flour, lignin, and cellulose," *Appl. Surf. Sci.* 317, 385-392. DOI: 10.1016/j.apsusc.2014.08.140
- Peng, Y., Liu, R., Cao, J., and Guo, X. (2015). "Effects of vitamin E combined with antioxidants on wood flour/polypropylene composites during accelerated weathering," *Holzforschung* 69(1), 113-120. DOI: 10.1515/hf-2014-0044
- Ratanawilai, T., and Taneerat, K. (2018). "Alternative polymeric matrices for wood-plastic composites: Effects on mechanical properties and resistance to natural weathering," *Constr. Build. Mater.* 172, 349-357. DOI: 10.1016/j.conbuildmat.2018.03.266
- Stark, N. M., and Matuana, L. M. (2004). "Surface chemistry and mechanical property changes of wood-flour/high-density-polyethylene composites after accelerated weathering," *J. Appl. Polym. Sci.* 94(6), 2263-2273. DOI: 10.1002/app.20996
- Stark, N. M., and Matuana, L. M. (2007). "Characterization of weathered wood-plastic composite surfaces using FTIR spectroscopy, contact angle, and XPS," *Polym. Degrad. Stabil.* 92(10), 1883-1890. DOI: 10.1016/j.polymdegradstab.2007.06.017
- Stark, N. M., Matuana, L. M., and Clemons, C. M. (2004). "Effect of processing method on surface and weathering characteristics of wood-flour/HDPE composites," *J. Appl. Polym. Sci.* 93(3), 1021-1030. DOI: 10.1002/app.20529
- Stark, N. M., and Rowlands, R. E. (2003). "Effect of wood fiber characteristics on mechanical properties of wood/polypropylene composites," *Wood Fiber Sci.* 35(2), 167-174.
- Takatani, M., Ito, H., Ohsugi, S., Kitayama, T., Saegusa, M., Kawai, S., and Okamoto, T. (2000). "Effect of lignocellulosic materials on the properties of thermoplastic polymer/wood composites," *Holzforschung* 54(2), 197-200. DOI: 10.1515/HF.2000.033
- Turku, I., and Kärki, T. (2016). "Accelerated weathering of fire-retarded wood-polypropylene composites," *Compos. Part A-Appl. S* 81, 305-312. DOI: 10.1016/j.compositesa.2015.11.028
- Turku, I., Kärki, T., and Puurtinen, A. (2018). "Durability of wood plastic composites manufactured from recycled plastic," *Heliyon* 4(3), article e00559. DOI: 10.1016/j.heliyon.2018.e00559
- Valente, M., Sarasini, F., Marra, F., Tirillo, J., and Pulci, G. (2011). "Hybrid recycled glass fiber/wood flour thermoplastic composites: Manufacturing and mechanical characterization," *Compos. Part A-Appl. S* 42(6), 649-657. DOI: 10.1016/j.compositesa.2011.02.004
- Wolcott, M. P. (2003). "Formulation and process development of flat-pressed wood-polyethylene composites," *Forest Prod. J.* 53(9), 25-32.

- Yang, T.-H., Yang, T.-H., Chao, W.-C., and Leu, S.-Y. (2015). "Characterization of the property changes of extruded wood–plastic composites during year round subtropical weathering," *Constr. Build. Mater.* 88, 159-168. DOI: 10.1016/j.conbuildmat.2015.04.019
- Yao, F., Wu, Q., Lei, Y., and Xu, Y. (2008). "Rice straw fiber-reinforced high-density polyethylene composite: Effect of fiber type and loading," *Ind. Crop Prod.* 28(1), 63-72. DOI: 10.1016/j.incrop.2008.01.007

Article submitted: May 3, 2023; Peer review completed: June 10, 2023; Revised version received and accepted: July 21, 2023; Published: July 28, 2023.
DOI: 10.15376/biores.18.3.6348-6363